Carbon-depleted outer core revealed by sound velocity measurements of liquid iron-carbon alloy

nature COMMUNICATIONS

ARTICLE

Received 30 May 2015 | Accepted 19 Oct 2015 | Published 24 Nov 2015

DOI: 10.1038/ncomms9942 OPEN

Carbon-depleted outer core revealed by sound velocity measurements of liquid iron–carbon alloy

Yoichi Nakajima[1], Saori Imada[2,3], Kei Hirose[3,4], Tetsuya Komabayashi[2,5], Haruka Ozawa[4,6], Shigehiko Tateno[3,6], Satoshi Tsutsui[7], Yasuhiro Kuwayama[8] & Alfred Q.R. Baron[1,7]

The relative abundance of light elements in the Earth's core has long been controversial. Recently, the presence of carbon in the core has been emphasized, because the density and sound velocities of the inner core may be consistent with solid Fe_7C_3. Here we report the longitudinal wave velocity of liquid $Fe_{84}C_{16}$ up to 70 GPa based on inelastic X-ray scattering measurements. We find the velocity to be substantially slower than that of solid iron and Fe_3C and to be faster than that of liquid iron. The thermodynamic equation of state for liquid $Fe_{84}C_{16}$ is also obtained from the velocity data combined with previous density measurements at 1 bar. The longitudinal velocity of the outer core, about 4% faster than that of liquid iron, is consistent with the presence of 4–5 at.% carbon. However, that amount of carbon is too small to account for the outer core density deficit, suggesting that carbon cannot be a predominant light element in the core.

[1] Materials Dynamics Laboratory, RIKEN SPring-8 Center, RIKEN, Hyogo 679-5148, Japan. [2] Department of Earth and Planetary Sciences, Tokyo Institute of Technology, Tokyo 152-8551, Japan. [3] Earth-Life Science Institute, Tokyo Institute of Technology, Tokyo 152-8550, Japan. [4] Laboratory of Ocean-Earth Life Evolution Research, Japan Agency for Marine-Earth Science and Technology, Kanagawa 237-0061, Japan. [5] School of GeoSciences and Centre for Science at Extreme Conditions, University of Edinburgh, Edinburgh EH9 3FE, UK. [6] Institute for Study of the Earth's Interior, Okayama University, Tottori 682-0193, Japan. [7] Research and Utilization Division, SPring-8, Japan Synchrotron Radiation Research Institute, Hyogo 679-5198, Japan. [8] Geodynamics Research Center, Ehime University, Ehime 790-8577, Japan. Correspondence and requests for materials should be addressed to Y.N. (email: yoichi.nakajima@spring8.or.jp).

Sound velocity and density are important observational constraints on the chemical composition of the Earth's core. While properties of solid iron alloys have been extensively examined by laboratory studies to core pressures (>136 GPa)[1–3], little is known for liquid alloys because of experimental difficulties. The core is predominantly molten, and the longitudinal wave (P-wave) velocity of liquid iron alloy is the key to constraining its composition. However, previous static high-pressure and -temperature (P–T) measurements of liquid iron alloys were performed only below 10 GPa using large-volume presses[4–6]. Shock wave experiments have been carried out at much higher pressures but only along a specific Hugoniot P–T path[7,8].

Carbon is one of the possible light alloying components in the core because of its high cosmic abundance and strong chemical affinity with liquid iron[9]. Its high metal/silicate partition coefficients indicate that thousands of parts per million to several weight percent of carbon could have been incorporated into the core during its formation[9–11]. In addition, recent experimental and theoretical studies[12,13] have suggested that solid Fe_7C_3 may explain the properties of the inner core, in particular its high Poisson's ratio[14,15], supporting the presence of carbon in the core.

In this study, we determine the P-wave velocity (V_P) (equivalent to bulk sound velocity, V_Φ, in a liquid) of liquid $Fe_{84}C_{16}$ at high P–T based on inelastic X-ray scattering (IXS) measurements. Combined with its density data at 1 bar (ref. 16) both velocity and density (ρ) profiles of liquid $Fe_{84}C_{16}$ along adiabatic compression are obtained. They are compared with seismological observations, indicating that both V_P and ρ in the Earth's outer core are not explained simultaneously by liquid Fe–C.

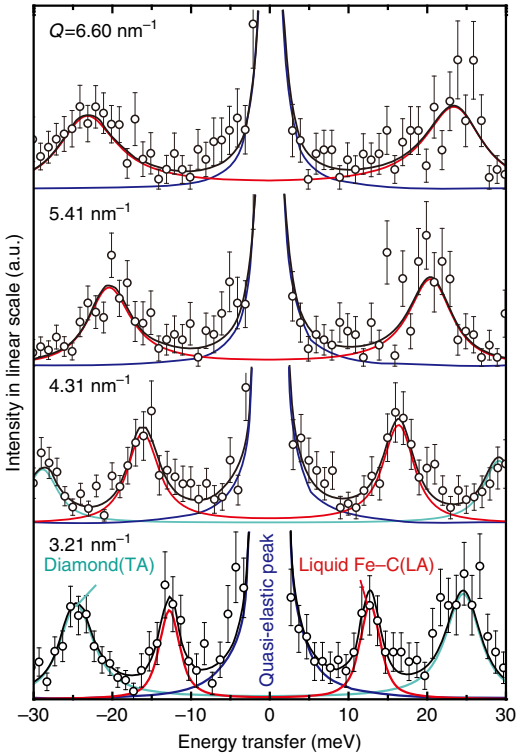

Figure 1 | Typical inelastic X-ray scattering spectra. These data were collected at 26 GPa and 2,530 K at momentum transfers Q, as indicated. The spectra include three components: a quasi-elastic peak near zero energy transfer (blue), longitudinal acoustic (LA) phonon mode of liquid $Fe_{84}C_{16}$ (red), and transverse acoustic (TA) phonon mode of diamond (turquoise).

Results

Longitudinal wave velocity measurements. We collected the high-resolution IXS spectra from liquid $Fe_{84}C_{16}$ (4.0 ± 0.3 wt.% carbon) at static high P–T using both resistance- and laser-heated diamond-anvil cells (Methods; Fig. 1). The starting material was synthesized beforehand as a mixture of fine-grained Fe and Fe_3C at 5 GPa and 1,623 K in a multi-anvil apparatus. Experimental P–T conditions were well above the eutectic temperature in the Fe–Fe_3C binary system (Supplementary Fig. 1). The carbon concentration in the eutectic liquid is known to be 3.8–4.3 wt.% at 1 bar to 20 GPa (ref. 17), almost identical to the composition of our sample. Above 20 GPa, we heated the sample to temperatures comparable or higher than the melting temperature of Fe_3C, a liquidus phase in the pressure range explored, assuring a fully molten sample. The molten state of the specimen was carefully confirmed, before and after the IXS measurements, by the absence of diffraction peaks from the sample (Fig. 2). We sometimes, depending on a sample volume, were also able to observe the diffuse diffraction signal typical of a liquid.

The V_P of liquid $Fe_{84}C_{16}$ was determined between 7.6 and 70 GPa (Fig. 3 and Supplementary Table 1) from dispersion curves for a range of momentum transfer (Fig. 4). It was found to be 15–30% smaller than that of solid Fe (refs 3,18–20) and Fe_3C (refs 21–23; note that a starting material in the present experiments was a mixture of these solid phases) (Fig. 5), confirming that we measured a liquid sample. The velocities of a fictive solid $Fe_{84}C_{16}$ alloy are also estimated assuming a linear velocity change between Fe (ref. 24) and Fe_3C (ref. 23) indicating that V_P drops by 13% upon melting at 2,300 K, a eutectic temperature at 45 GPa (ref. 17). Such a velocity change is comparable to that expected for pure Fe. The difference in V_Φ between solid and liquid $Fe_{84}C_{16}$ is very small (1.8%). On the other hand, the V_P of our liquid $Fe_{84}C_{16}$ sample is 3–14% faster at 8–70 GPa than that of liquid Fe determined by shock-wave study[8] (Fig. 3).

Earlier ultrasonic measurements performed below 10 GPa reported a change in V_P by <2–3% per 1,000 K for liquid Fe–S alloys[4,5]. Theoretical calculations[25–27] and shock compression data[8] on liquid Fe and Fe–S alloy demonstrated even smaller effects above 100 GPa (<0.5% by 1,000 K). It is therefore very likely that the V_P of liquid $Fe_{84}C_{16}$ is also not sensitive to temperature with the temperature effect much smaller than the uncertainty in the present velocity determinations (±3%).

Thermodynamical equation of state. V_P of a liquid can be described using the Murnaghan equation of state[4] (Methods) as;

$$V_P = \sqrt{\frac{K_{S0}}{\rho_0}}\left(1+\frac{K'_S}{K_{S0}}P\right)^{\frac{1}{2}-\frac{1}{2K'_S}}, \quad (1)$$

where K_S and K'_S are adiabatic bulk modulus and its pressure derivative, respectively (zero subscripts denote values at 1 bar and $T=T_0$). Here, consistent with the discussion above, we neglect the temperature dependence of our V_P data, while ρ_0 is taken to be temperature dependent[16] (Methods). We fit equation (1) to our P–V_P data for liquid $Fe_{84}C_{16}$ and find $K_{S0}=110\pm9$ GPa and $K'_S=5.14\pm0.30$ when $T_0=2{,}500$ K (Supplementary Table 2 and Supplementary Fig. 2). The choice of T_0 and, accordingly, the variation in ρ_0 practically changed K_{S0} and K'_{S0} as $(\partial K_{S0}/\partial T)=-9.4\times10^{-3}$ GPa K^{-1} and $(\partial K'_{S0}/\partial T)=-2.7\times10^{-4}$ K^{-1}. Our value for K_{S0} is similar to that for liquid iron[8] but for K'_S is higher than that for pure iron, $K'_S=4.7$.

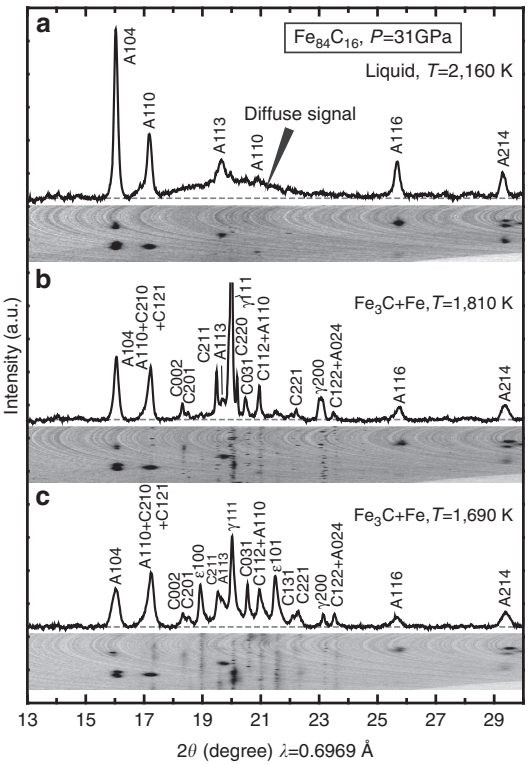

Figure 2 | X-ray diffraction spectra before and after melting. They were collected at 2,160 K (**a**), 1,810 K (**b**) and 1,690 K (**c**) during heating at 31 GPa. The starting material was composed of Fe (ε or γ) and Fe_3C (**c**), and the peaks of Al_2O_3 (**a**) were from a thermal insulator. The coexistence of ε- and γ-Fe phases at 1,610 K was due to a sluggish solid–solid phase transition[49] and the peaks from the ε-phase were lost at 1,810 K. All sample peaks disappeared between 1,810 and 2,160 K. In addition, the background was enhanced slightly, indicating a diffuse scattering signal from a liquid sample.

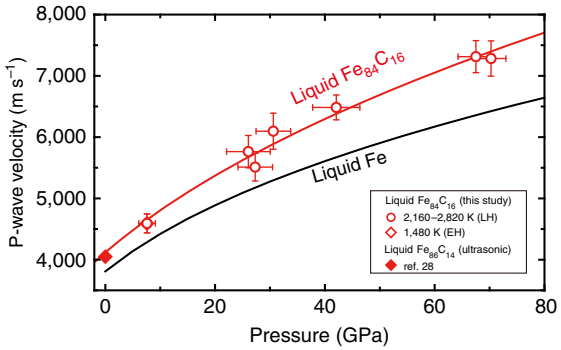

Figure 3 | Compressional wave velocity of liquid $Fe_{84}C_{16}$. Open circles, obtained by laser-heated DAC; open diamond, by external-resistance-heated DAC. The data at 1 bar is from ultrasonic measurements[28] (closed diamond). The red curve represents a thermodynamical fitting result for liquid $Fe_{84}C_{16}$, compared with the velocity of liquid Fe (black curve)[8].

This suggests that liquid $Fe_{84}C_{16}$ becomes progressively stiffer than liquid Fe with increasing pressure. We also found $V_{P0} = 4{,}121 \pm 177\,m\,s^{-1}$ for liquid $Fe_{84}C_{16}$ from K_{S0} and ρ_0, in good agreement with a previous study[28] of liquid $Fe_{86}C_{14}$ at 1 bar ($4{,}050\,m\,s^{-1}$) and faster than $V_{P0} = 3{,}860\,m\,s^{-1}$ for liquid Fe (ref. 8).

To compare the present results with earlier density measurements of liquid Fe–C alloys at high pressure[29,30] the isothermal bulk modulus for liquid $Fe_{84}C_{16}$ is estimated to be $K_{T0} = 100$ (82) GPa at 1,500 K (2,500 K) from our determination of K_S combined with Grüneisen parameter $\gamma_0 = 1.74$ (ref. 8) and

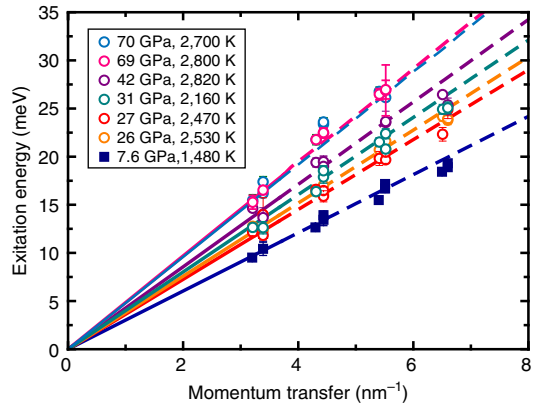

Figure 4 | Longitudinal acoustic phonon dispersion of liquid $Fe_{84}C_{16}$. The dispersion data were obtained at pressures from 7.6 to 70 GPa. Only data collected with the low momentum transfer ($<3.5\,nm^{-1}$) were used to determine the velocity to avoid possible anomalous dispersion for liquid (see Methods).

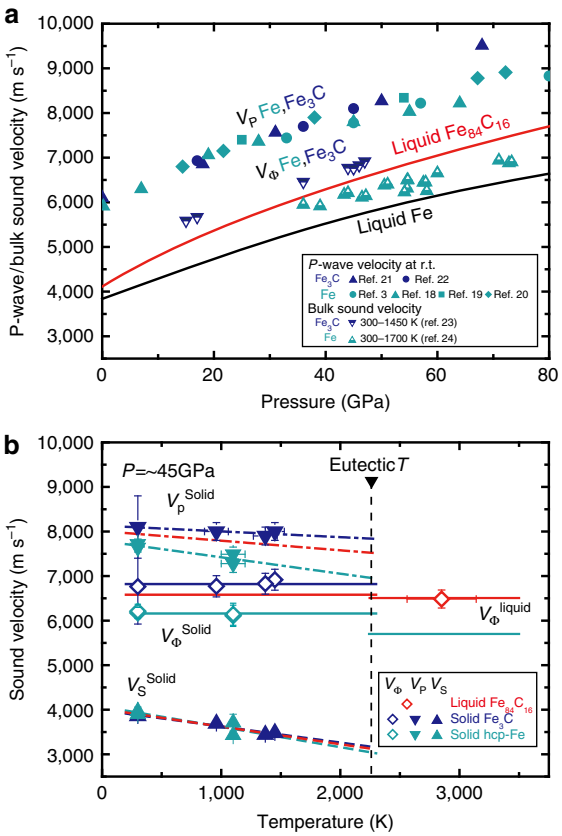

Figure 5 | Comparison of velocities between liquid and solid Fe–C alloys. (**a**), P-wave velocities (V_P) and bulk sound velocities (V_Φ) of solid Fe (turquoise)[3,18–20,24] and Fe_3C (blue)[21–23] were determined by previous IXS and nuclear inelastic scattering (NIS) measurements. The V_P for liquid Fe is from shock-wave study[8]. (**b**), Temperature effects on the sound velocities of Fe–C alloys at ~45 GPa. The V_P (= V_Φ) of liquid $Fe_{84}C_{16}$ and liquid Fe is from the present work at 42 GPa and shock-wave data[8], respectively. The V_P, shear velocity (V_S), and V_Φ for solid Fe and Fe_3C were reported by NIS measurements[23,24]. Red lines for fictional solid $Fe_{84}C_{16}$ are estimated from a linear relationship between Fe and Fe_3C.

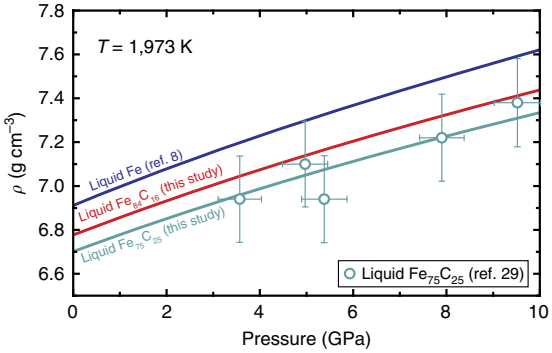

Figure 6 | Comparison with previous density measurements. Blue and red curves demonstrate calculated densities at 1,973 K for liquid Fe (ref. 8) and $Fe_{84}C_{16}$ (present study). The density of liquid $Fe_{75}C_{25}$ (turquoise curve) is estimated assuming linear compositional dependence between pure Fe and $Fe_{75}C_{25}$, which shows good agreement with the previous measurements at 1,973 K (ref. 29).

thermal expansion coefficient[16] (Methods). When applying $C_P/C_V = 1.125$ at 1,820 K for liquid $Fe_{86}C_{14}$ derived from theoretical calculations[31], $K_{T0} = 106$–98 GPa is obtained at the same temperature range. These K_{T0} values for liquid $Fe_{84}C_{16}$ are similar to $K_{T0} = 95$–63 GPa for liquid Fe at 1,500–2,500 K (ref. 8) On the other hand, they are significantly larger than $K_{T0} = 55.4$ GPa for liquid $Fe_{86}C_{14}$ at 1,500 K and $K_{T0} = 50$ GPa for liquid $Fe_{75}C_{25}$ at 1,973 K from previous density measurements[29,30]. However, the calculated density for $Fe_{84}C_{16}$ using the present EoS are in reasonable agreement with the previous density measurements of $Fe_{75}C_{25}$ (ref. 29) (Fig. 6). The disagreement of elastic parameters with such earlier experiments may be attributed either to the limited pressure range of the previous density determinations, or to a different structure or magnetic (or electronic) change in the state of the liquid Fe–C at low pressure, as has been suggested from the change in compressional behaviour of liquid $Fe_{78}C_{22}$ around 5 GPa (ref. 6). Our data were collected above 7.6 GPa, so that the physical properties of liquid Fe–C obtained here should be more applicable to the Earth's core.

ρ of liquid $Fe_{84}C_{16}$ is then given, using the elastic parameters determined above, by;

$$\rho = \rho_0 \left(1 + \frac{K_S'}{K_{S0}} P\right)^{\frac{1}{K_S'}}. \quad (2)$$

Equations (1) and (2) give the V_P and ρ profiles for adiabatic compression (Methods), assuming $\gamma_0 = 1.74$, the same as that of liquid Fe (ref. 8) (Fig. 7). We find $V_P = 9{,}200\ \mathrm{m\,s^{-1}}$ and $\rho = 9.82$–$9.61\ \mathrm{g\,cm^{-3}}$ at the core-mantle boundary (CMB) for $T_{CMB} = 3{,}600$–$4{,}300$ K (refs 32,33) This indicates that V_P of liquid $Fe_{84}C_{16}$ is 19.6% faster than that of liquid Fe at the CMB[8], implying that the addition of 1 at.% carbon increases the V_P of liquid Fe by 1.2%. The extrapolation of the present experimental data using the Murnaghan equation of state may overestimate the V_P by 2 − 4% at the CMB (Supplementary Note 1 and Supplementary Fig. 3), but, even if this is the case, 1 at.% carbon enhances the V_P of liquid Fe by as large as 0.8%. Indeed, the effect of carbon is much larger than a recent theoretical prediction of only 0.2% increase in velocity per 1 at.% carbon at 136 GPa (ref. 34). On the other hand, our data show that the incorporation of 1 at.% carbon reduces the density of liquid Fe by 0.6–0.7%, while theory suggested only 0.3% density reduction by 1 at.% carbon[34].

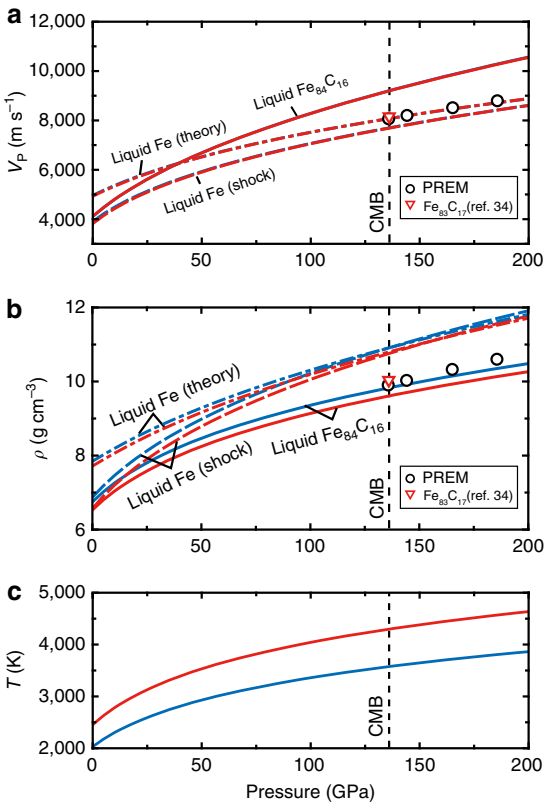

Figure 7 | Velocity and density of liquid $Fe_{84}C_{16}$ extrapolated to core pressures. The P-wave velocity (**a**) and density (**b**) profiles of liquid $Fe_{84}C_{16}$ are calculated along two adiabatic temperature curves (**c**) of 3,600 K (blue) and 4,300 K (red) at the CMB. Those for liquid Fe are from shock-compression experiments[8] and theoretical calculations[26]. The velocity and density for liquid $Fe_{83}C_{17}$ at the CMB (4,300 K) are by theory[34]. PREM denotes seismologically deduced Preliminary Reference Earth model[35].

Discussion

We now compare the sound velocity and density of liquid $Fe_{84}C_{16}$ and liquid Fe with the seismologically based PREM model[35] for the outer core (Fig. 8). The V_P and ρ of liquid Fe are 4.6% slower and 10.1–8.6% denser, respectively, than the PREM at the CMB (3,600–4,300 K). To match the PREM values, considering the uncertainty of data extrapolation to higher pressures (Supplementary Note 1), only 5.2–4.0 at.% (1.2–0.9 wt.%) carbon is required to match the velocity, whereas 15.4–12.0 at.% (3.8–2.9 wt.%) carbon is necessary to account for the density. Therefore, carbon cannot be a predominant light element in the outer core.

These results suggest there is <5.2 at.% (1.2 wt.%) carbon in the outer core, consistent with the previous cosmochemical and geochemical arguments. In particular, the silicate portion of the Earth exhibits much higher $^{13}C/^{12}C$ isotopic ratio than that of Mars, Vesta and chondrite meteorites, as may be attributed to a strong enrichment of ^{12}C in core-forming metals[9]. The carbon isotopic fractionation that occurred during continuous core-formation process proposed previously[36,37] will give a reasonable $^{13}C/^{12}C$ ratio in the silicate Earth, and yields 1 wt.% carbon in the core[9]. In addition, Wood *et al.*[9] demonstrated that carbon strongly affects the chemical activity of Mo and W in liquid metal, so that their abundance in the mantle can be explained by partitioning between silicate melt and core-forming metal with ∼0.6 wt.% carbon. It has been repeatedly suggested that the inner core may be composed of Fe_7C_3, which accounts

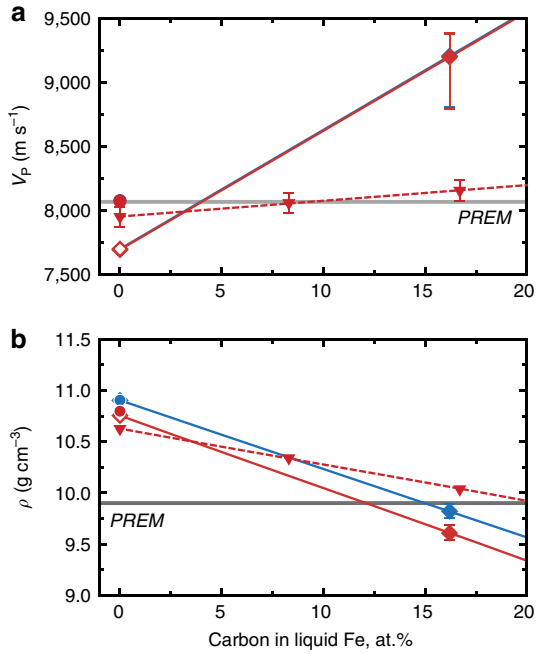

Figure 8 | Effect of carbon on the velocity and density of liquid Fe at 136 GPa. (**a**) Velocity and (**b**) density for liquid $Fe_{84}C_{16}$ at $T_{CMB}=4{,}300$ K (red) and 3,600 K (blue). Present results (closed diamonds, solid curves) are compared with theoretical calculations[34] (triangles, broken curve). The data for pure Fe are from shock compression study[8] (open diamonds) and theoretical calculations[26] (closed circles). PREM denotes seismological observations[35] at the CMB.

for high Poisson's ratio observed[14,15]. The crystallization of solid Fe_7C_3 from a liquid outer core with <1.2 wt.% carbon may still be possible if sulfur is also included in the core[38].

Methods

High *P–T* generation. Molten Fe–C alloy was obtained at high *P–T* in an external-resistance-heated (EH) or laser-heated (LH) diamond-anvil cell (DAC; Supplementary Table 1) using facilities installed at SPring-8. A disc of pre-synthesized $Fe_{84}C_{16}$ sample, 20–25 μm thick and 100–120 μm in diameter, was loaded into a hole of a rhenium gasket, together with two 12–17 μm thick single-crystal Al_2O_3 sapphire discs that served as both thermal and chemical insulators. The sample was compressed with 300 μm culet diamond anvils to a pressure of interest before heating.

In LH-DAC experiments, the sample was heated at high pressure from both sides by using two 100 W single-mode Yb fibre lasers (YLR-100-AC, IPG Photonics Corp.). The Gaussian-type energy distribution of the laser beam was converted into flat-top one with a refractive beam shaper (GBS-NIR-H3, Newport Corp.). A typical laser spot was 50–70 μm in diameter on the sample, much larger than X-ray beam size ($\sim$17 μm). We determined temperature by a spetroradiometric method, and its variations within the area irradiated by X-rays and fluctuations during IXS measurements were $<\pm10\%$. The pressure was obtained from the equation of state for Fe_3C (ref. 39) from the lattice constant observed before melting at 1,800–2,500 K. Its error was derived from uncertainties in both temperature and the volume of Fe_3C. A typical image of a sample recovered after the laser heating experiment at 70 GPa and 2,700 K is given in Supplementary Fig. 4.

Only run #FeC08 was conducted in an EH-DAC. The whole sample was homogeneously heated by a platinum-resistance heater placed around the diamonds. The temperature was obtained with a Pt-Rh (type-R) thermocouple whose junction was in contact with the diamond near a sample chamber. The temperature uncertainty was <20 K. We determined the pressure based on the Raman shift of a diamond anvil[40] before heating at 300 K, whose uncertainty may be as much as $\pm20\%$.

IXS measurements. The sound velocity of liquid Fe–C alloy was determined in the DAC by high-resolution IXS spectroscopy at the beamline BL35XU, SPring-8 (ref. 41). Both LH- and EH-DACs were placed into vacuum chambers to minimize background scattering by air. The measurements were carried out with $\sim$2.8 meV energy resolution using Si (999) backscattering geometry at 17.79 keV. The experimental energy resolutions were determined using scattering from Polymethyl–methacrylate. The incident X-ray beam was focused to about 17 μm size (full width at half maximum) in both horizontal and vertical directions by using Kirkpatrick–Baez mirrors[42]. The X-ray beam size was much smaller than heated area (50–70 μm for LH-DAC). Scattered photons were collected by an array of 12 spherical Si analyzers leading to 12 independent spectra at momentum transfers (Q) between 3.2 and 6.6 nm^{-1} with a resolution $\Delta Q\sim0.45$ nm^{-1} (full width) that was set by slits in front of the analyzer array. The energy transfer range of ±30 (or -10 to ±30) meV was scanned for 1–3 h. Before and after IXS data collections, sample melting was confirmed by X-ray diffraction data (Fig. 2) that was collected, *in situ*, by switching a detector to a flat panel area detector (C9732DK, Hamamatsu Photonics K.K.)[43].

The IXS spectra included three (sometimes five) peaks (Fig. 1) of Stokes and anti-Stokes components of the longitudinal acoustic (LA) phonon mode from the sample (sometimes also from a diamond), and a quasi-elastic contribution near zero energy transfer. These spectra were fitted with the damped harmonic oscillator (DHO) mode[44] for acoustic phonon modes and with Lorenzian function for quasi-elastic peaks convolved by experimental resolution function. The DHO model function can be described as;

$$S^{\mathrm{DHO}}(Q,\omega)=\left[\frac{1}{1-e^{-\hbar\omega/k_BT}}\right]\frac{A_Q}{\pi}\frac{4\omega\omega_Q\gamma_Q}{(\omega^2-\Omega_Q^2)^2+4\gamma_Q^2\omega^2}, \quad (3)$$

where A_Q, Γ_Q, Ω_Q, k_B and $\hbar$ are the amplitude, width, and energy of inelastic modes, Boltzmann constant and Planck constant, respectively. In the fitting, temperature T was fixed at a sample temperature obtained by a spetroradiometric method or a thermocouple. The excitation energy modes appearing at both Stokes and anti-Stokes sides correspond to the phonon creation and annihilation, respectively. With increasing temperature, as given by the Bose function in equation (3), the intensities of such Stokes and anti-Stokes peaks become similar to each other. A symmetric shape of the present IXS spectra therefore assures that the IXS signals originated from a high-temperature area.

The peak at a finite energy transfer gives the frequency of each mode (Fig. 1). The excitation energies for the LA phonon mode of liquid $Fe_{84}C_{16}$ obtained in a pressure range of 7.6–70 GPa are plotted as a function of momentum transfer (Q) in Fig. 4. The compressional sound wave or P-wave velocity (V_P) corresponds to the long-wavelength LA velocity at $Q\rightarrow0$ limits;

$$V_P=\left(\frac{dE}{dQ}\right)_{Q\rightarrow0}. \quad (4)$$

We made a linear fit to the data obtained at low Q below 3.5 nm^{-1} to determine the P-wave velocity (Supplementary Table 1), because positive dispersion can appear at higher $Q\gg3$ nm^{-1} (ref. 45). For comparison, the results based on a sine-curve fit to all Q-range data, as is usually applied for polycrystalline samples in similar high-pressure IXS measurements[46], are also given in Supplementary Table 1. In general, the error bars of the two determinations of V_P overlap, though the sine fit to large Q does give slightly larger V_P, as would qualitatively be expected from previous measurements on liquid iron[47].

Equation of state for liquid $Fe_{84}C_{16}$. We constructed an equation of state (EoS) for liquid $Fe_{84}C_{16}$ to extrapolate the present V_P data and to estimate its density at the core pressure range. V_P of liquid can be written as;

$$V_P=\sqrt{\frac{K_S}{\rho}}. \quad (5)$$

The pressure dependence of K_S is assumed to be

$$K_S=K_{S0}+K_S'P, \quad (6)$$

where K'_S is the pressure derivative of K_S and pressure and subscript zero indicates a value at 1 bar. The adiabatic Murnaghan EoS can be described as (for example, ref. 4);

$$\rho=\rho_0\left(1+\frac{K_S'}{K_{S0}}P\right)^{\frac{1}{K_S'}}. \quad (7)$$

Equation (5) is thus rewritten as;

$$V_P=\sqrt{\frac{K_{S0}}{\rho_0}}\left(1+\frac{K_S'}{K_{S0}}P\right)^{\frac{1}{2}-\frac{1}{2K_S'}}. \quad (8)$$

The temperature effect on ρ_0 can be expressed by;

$$\rho_0(T)=\rho_0(T_0)/\exp\left(\int_{T_0}^{T}\alpha dT\right). \quad (9)$$

The thermal expansion coefficient α is also dependent on temperature as;

$$\alpha(T)=a+bT, \quad (10)$$

where a and b are constants. Previous density measurements[16] of liquid Fe–C alloys at 1 bar give $a=6.424\times10^{-5}$ K^{-1} and $b=0.606\times10^{-8}$ K^{-2} for liquid

$Fe_{84}C_{16}$ using $\rho_0 = 6.505\,g\,cm^{-3}$ at $T_0 = 2{,}500$ K as a reference. The result of fitting equation (8) to the present $P - V_P$ data is given in Fig. 3.

Isothermal bulk modulus. We estimate isothermal bulk modulus K_T from isentropic bulk modulus K_S in two ways. The relationship between these two is described as follows;

$$\frac{K_S}{K_T} = \frac{C_P}{C_V} = 1 + \alpha\gamma, \tag{11}$$

where C_P and C_V are heat capacities at constant pressure and volume, respectively. Although γ for liquid Fe–C alloys is not known, $\gamma_0 = 1.74$ has been reported for liquid Fe at 1 bar and 1,811 K (ref. 8) It is close to 1.58 for liquid $Fe_{90}O_8S_2$ estimated from the shock compression data set[48].

Extrapolation of present data to core pressures. With the EoSs determined above (equations (7) and (8)), we extrapolate the P-wave velocity and density of liquid $Fe_{84}C_{16}$ to the core pressure range along adiabatic compression, in which temperature is given by;

$$T = T_0 \exp\left[\int_{\rho_0}^{\rho} (\gamma/\rho)d\rho\right]. \tag{12}$$

Assuming $\gamma = \gamma_0 \times (\rho_0/\rho)$, temperature is simply represented as;

$$T = T_0 \exp\left[\gamma_0\left(1 - \frac{\rho_0}{\rho}\right)\right]. \tag{13}$$

γ_0 is fixed at 1.74 previously obtained for liquid Fe (ref. 8). Using the temperature dependence of K_{S0} and ρ_0 shown above, we calculate density, velocity and temperature profiles along adiabatic compression with various reference temperatures at the CMB. The adiabatic compression profiles of liquid $Fe_{84}C_{16}$ for the low ($T_0 = 2{,}045$ K and $T_{CMB} = 3{,}600$ K)[32] and high ($T_0 = 2{,}457$ K and $T_{CMB} = 4{,}300$ K)[33] temperature cases are calculated in Fig. 7.

References

1. Badro, J. *et al.* Effect of light elements on the sound velocities in solid iron: implications for the composition of Earth's core. *Earth Planet. Sci. Lett.* **254,** 233–238 (2007).
2. Sata, N. *et al.* Compression of FeSi, Fe_3C, $Fe_{0.95}O$, and FeS under the core pressures and implication for light element in the Earth's core. *J. Geophys. Res.* **115,** B09204 (2010).
3. Ohtani, E. *et al.* Sound velocity of hexagonal close-packed iron up to core pressures. *Geophys. Res. Lett.* **40,** 5089–5094 (2013).
4. Jing, Z. *et al.* Sound velocity of Fe-S liquids at high pressure: implications for the Moon's molten outer core. *Earth Planet. Sci. Lett.* **396,** 78–87 (2014).
5. Nishida, K. *et al.* Sound velocity measurements in liquid Fe-S at high pressure: Implications for Earth's and lunar cores. *Earth Planet. Sci. Lett.* **362,** 182–186 (2013).
6. Sanloup, C., van Westrenen, W., Dasgupta, R., Maynard-Casely, H. & Perrillat, J.-P. Compressibility change in iron-rich melt and implications for core formation models. *Earth Planet. Sci. Lett.* **306,** 118–122 (2011).
7. Huang, H. *et al.* Evidence for an oxygen-depleted liquid outer core of the Earth. *Nature* **479,** 513–516 (2011).
8. Anderson, W. W. & Ahrens, T. J. An equation of state for liquid iron and implications for the Earth's core. *J. Geophys. Res.* **99,** 4273–4284 (1994).
9. Wood, B. J., Li, J. & Shahar, A. Carbon in the core: its influence on the properties of core and mantle. *Rev. Miner. Geochem* **75,** 231–250 (2013).
10. Chi, H., Dasgupta, R., Duncan, M. S. & Shimizu, N. Partitioning of carbon between Fe-rich alloy melt and silicate melt in a magma ocean – implications for the abundance and origin of volatiles in Earth, Mars, and the Moon. *Geochim. Cosmochim. Acta* **139,** 447–471 (2014).
11. Nakajima, Y., Takahashi, E., Suzuki, T. & Funakoshi, K. "Carbon in the core" revisited. *Phys. Earth Planet. In.* **174,** 202–211 (2009).
12. Nakajima, Y. *et al.* Thermoelastic property and high-pressure stability of Fe_7C_3: implication for iron-carbide in the Earth's core. *Am. Mineral.* **96,** 1158–1165 (2011).
13. Mookherjee, M. *et al.* High-pressure behavior of iron carbide (Fe_7C_3) at inner core conditions. *J. Geophys. Res.* **116,** B04201 (2011).
14. Prescher, C. *et al.* High Poisson's ratio of Earth's inner core explained by carbon alloying. *Nat. Geosci.* **8,** 220–223 (2015).
15. Chen, B. *et al.* Hidden carbon in Earth's inner core revealed by shear softening in dense Fe_7C_3. *Proc. Natl Acad. Sci. USA* **111,** 17755–17758 (2014).
16. Ogino, K., Nishiwaki, A. & Hosotani, Y. Density of molten Fe-C alloys. *J. Jpn Inst. Met.* **48,** 1004–1010 (1984).
17. Fei, Y. & Brosh, E. Experimental study and thermodynamic calculations of phase relations in the Fe-C system at high pressure. *Earth Planet. Sci. Lett.* **408,** 155–162 (2014).
18. Fiquet, G., Badro, J., Guyot, F., Requardt, H. & Krisch, M. Sound velocities in iron to 110 gigapascals. *Science* **291,** 468–471 (2001).
19. Antonangeli, D. *et al.* Simultaneous sound velocity and density measurements of hcp iron up to 93 GPa and 1100 K: an experimental test of the Birch's law at high temperature. *Earth Planet. Sci. Lett.* **331-332,** 210–214 (2012).
20. Mao, Z. *et al.* Sound velocities of Fe and Fe-Si alloy in the Earth's core. *Proc. Natl Acad. Sci. USA* **109,** 10239–10244 (2012).
21. Fiquet, G., Badro, J., Gregoryanz, E., Fei, Y. & Occelli, F. Sound velocity in iron carbide (Fe_3C) at high pressure: implications for the carbon content of the Earth's inner core. *Phys. Earth Planet. In.* **172,** 125–129 (2009).
22. Gao, L. *et al.* Sound velocities of compressed Fe_3C from simultaneous synchrotron X-ray diffraction and nuclear resonant scattering measurements. *J. Synchrotron Radiat.* **16,** 714–722 (2009).
23. Gao, L. *et al.* Effect of temperature on sound velocities of compressed Fe_3C, a candidate component of the Earth's inner core. *Earth Planet. Sci. Lett.* **309,** 213–220 (2011).
24. Lin, J. *et al.* Sound velocities of hot dense iron: Birch's law revisited. *Science* **308,** 1892–1894 (2005).
25. Vočadlo, L., Alfè, D., Gillan, M. J. & Price, G. D. The properties of iron under core conditions from first principles calculations. *Phys. Earth Planet. In.* **140,** 101–125 (2003).
26. Ichikawa, H., Tsuchiya, T. & Tange, Y. The P-V-T equation of state and thermodynamic properties of liquid iron. *J. Geophys. Res. Solid Earth* **119,** 240–252 (2014).
27. Umemoto, K. *et al.* Liquid iron-sulfur alloys at outer core conditions by first-principles calculations. *Geophys. Res. Lett.* **41,** 6712–6717 (2014).
28. Pronin, L., Kazakov, N. & Filippov, S. Ultrasonic measurements in molten iron. *Izv. Vuzov. Chernaya Metall* **5,** 12–16 (1964).
29. Terasaki, H. *et al.* Density measurement of Fe_3C liquid using X-ray absorption image up to 10 GPa and effect of light elements on compressibility of liquid iron. *J. Geophys. Res.* **115,** B06207 (2010).
30. Shimoyama, Y. *et al.* Density of Fe-3.5wt% C liquid at high pressure and temperature and the effect of carbon on the density of the molten iron. *Phys. Earth Planet. In.* **224,** 77–82 (2013).
31. Belashchenko, D. K., Mirzoev, A. & Ostrovski, O. Molecular dynamics modelling of liquid Fe-C alloys. *High Temp. Mater. Processess* **30,** 297–303 (2011).
32. Nomura, R. *et al.* Low core-mantle boundary temperature inferred from the solidus of pyrolite. *Science* **343,** 522–525 (2014).
33. Anzellini, S., Dewaele, A., Mezouar, M., Loubeyre, P. & Morard, G. Melting of iron at Earth's inner core boundary based on fast X-ray diffraction. *Science* **340,** 464–466 (2013).
34. Badro, J., Côté, A. S. & Brodholt, J. P. A seismologically consistent compositional model of Earth's core. *Proc. Natl Acad. Sci. USA* **111,** 7542–7545 (2014).
35. Dziewonski, A. M. & Anderson, D. L. Preliminary reference Earth model. *Phys. Earth Planet. In.* **25,** 297–356 (1981).
36. Wood, B. J., Walter, M. J. & Wade, J. Accretion of the Earth and segregation of its core. *Nature* **441,** 825–833 (2006).
37. Rubie, D. C. *et al.* Heterogeneous accretion, composition and core–mantle differentiation of the Earth. *Earth Planet. Sci. Lett.* **301,** 31–42 (2011).
38. Wood, B. J. Carbon in the core. *Earth Planet. Sci. Lett.* **117,** 593–607 (1993).
39. Litasov, K. D. *et al.* Thermal equation of state and thermodynamic properties of iron carbide Fe_3C to 31 GPa and 1473 K. *J. Geophys. Res. Solid Earth* **118,** 5274–5284 (2013).
40. Akahama, Y. & Kawamura, H. Pressure calibration of diamond anvil Raman gauge to 310 GPa. *J. Appl. Phys.* **100,** 043516 (2006).
41. Baron, A. Q. R. *et al.* An X-ray scattering beamline for studying dynamics. *J. Phys. Chem. Solids* **61,** 461–465 (2000).
42. Ishikawa, D., Uchiyama, H., Tsutsui, S., Fukui, H. & Baron, A. Q. R. Compound focusing for hard x-ray inelastic scattering. *Proc. SPIE* 8848–88480F (2013).
43. Fukui, H. *et al.* A compact system for generating extreme pressures and temperatures: an application of laser-heated diamond anvil cell to inelastic X-ray scattering. *Rev. Sci. Instrum* **84,** 113902 (2013).
44. Fåk, B. & Dorner, B. Phonon line shapes and excitation energies. *Phys. B Condens. Matter* **234-236,** 1107–1108 (1997).
45. Scopigno, T., Ruocco, G. & Sette, F. Microscopic dynamics in liquid metals: the experimental point of view. *Rev. Mod. Phys.* **77,** 881–933 (2005).
46. Fiquet, G. *et al.* Application of inelastic X-ray scattering to the measurements of acoustic wave velocities in geophysical materials at very high pressure. *Phys. Earth Planet. In.* **143,** 5–18 (2004).
47. Hosokawa, S., Inui, M., Matsuda, K., Ishikawa, D. & Baron, A. Damping of the collective modes in liquid Fe. *Phys. Rev. B* **77,** 174203 (2008).
48. Huang, H. *et al.* Melting behavior of Fe-O-S at high pressure: a discussion on the melting depression induced by O and S. *J. Geophys. Res.* **115,** B05207 (2010).

49. Kubo, A. *et al.* In situ X-ray observation of iron using Kawai-type apparatus equipped with sintered diamond: absence of β phase up to 44 GPa and 2100 K. *Geophys. Res. Lett.* **30,** 1126 (2003).

Acknowledgements

We thank H. Fukui for his advice through IXS measurements. H. Uchiyama, D. Ishikawa, N. Murai and Y. Um are acknowledged for their supports during synchrotron experiments and data analyses, and D. Ishikawa and H. Fukui for implementation of the KB setup. Comments from three anonymous reviewers were helpful. All experiments were performed at BL35XU, SPring-8 (Proposal no. 2012B1356, 2013A1541, 2013B1407, 2014A1368, 2014B1271 and 2014B1536).

Author contributions

Y.N. synthesized a starting material and performed experiments and data analysis. Y.N., S.I., K.H, T.K., S. Tateno, S. Tsutsui, Y.K. and A.B. were involved in IXS measurements. H.O., S. Tateno, S.I. and Y.N. were involved in developing the laser heating system at the beamline. Y.N., K.H. and A.B. wrote the paper. All authors discussed the results and commented on the manuscript.

Additional information

Supplementary Information accompanies this paper at http://www.nature.com/naturecommunications

Competing financial interests: The authors declare no competing financial interests.

Reprints and permission information is available online at http://npg.nature.com/reprintsandpermissions/

How to cite this article: Nakajima, Y. *et al.* Carbon-depleted outer core revealed by sound velocity measurements of liquid iron–carbon alloy. *Nat. Commun.* 6:8942 doi: 10.1038/ncomms9942 (2015).